

Non-linear longitudinal fracture in a functionally graded beam

Victor I. Rizov*

*Department of Technical Mechanics, University of Architecture, Civil Engineering and Geodesy,
1 Chr. Smirnensky Blvd., 1046 - Sofia, Bulgaria*

(Received August 21, 2017, Revised December 11, 2017, Accepted February 5, 2018)

Abstract. Longitudinal fracture in a functionally graded beam configuration was studied analytically with taking into account the non-linear behavior of the material. A cantilever beam with two longitudinal cracks located symmetrically with respect to the centroid was analyzed. The material was functionally graded along the beam width as well as along the beam length. The fracture was studied in terms of the strain energy release rate. The influence of material gradient, crack location along the beam width, crack length and material non-linearity on the fracture behavior was investigated. It was shown that the analytical solution derived is very useful for parametric analyses of the non-linear longitudinal fracture behavior. It was found that by using appropriate material gradients in width and length directions of the beam, the strain energy release rate can be reduced significantly. Thus, the results obtained in the present paper may be applied for optimization of functionally graded beam structure with respect to the longitudinal fracture performance.

Keywords: functionally graded beam; fracture; material non-linearity; analytical solution

1. Introduction

The application of functionally graded materials has increased considerably for the last two decades in aerospace, electronics, optics, nuclear energy, engineering, etc. (Bohidar *et al.* 2014, Farzad Ebrahimi *et al.* 2016, Gasik 2010, Hadji *et al.* 2015, Hirai and Chen 1999, Koizumi 1993, Lu *et al.* 2009, Markworth, Ramesh and Parks 1995, Mortensen and Suresh 1995, Naser and Alahmad 2017, Nemat-Allal *et al.* 2011, Neubrand and Rödel 1997). This is due mainly to the fact that by gradual changing the material property distribution in one or more spatial directions during manufacturing process, one can meet requirements for various material properties in different parts of a structural member, which is the basic advantage of functionally graded materials over the traditional structural materials. Recently, interesting thermo-mechanical dynamic and buckling analyses of various functionally graded beam configurations (sandwich beams with functionally graded composite face sheets, functionally graded beams with porosities, nanosize beams and others) have been developed (Ebrahimi and Salari 2015, Ebrahimi and Farzamandnia 2016, Ebrahimi and Jafari 2016, Ebrahimi and Barati 2016a, b, c, d, e, f, g, Ebrahimi and Shafiei 2016). The concept of neutral axis has been discussed and applied by Ebrahimi and Salari (2015) for the case when the material is functionally graded along the beam height (along z -axis). In recent years,

*Corresponding author, Professor, E-mail: v_rizov_fhe@uacg.bg

important contributions in mechanics of functionally graded beams and plates have been done by Ait Amar Meziane *et al.* (2014), Ait Atmane *et al.* (2015), Bellifa *et al.* (2016), Bourada *et al.* (2015), Hadji (2017), Hadji *et al.* (2017). In structural applications of functionally graded materials, fracture is very often a critical failure mode that leads to lose of structural capacity and functionality. Therefore, fracture mechanics of these novel materials continues to attract the attention of researchers around the world (Brajesh Panigrahi and Goutam Pohit 2016, Carpinteri and Pugno 2006, Erdogan 1995, Lia-Liang *et al.* 2009, Paulino 2002, Rizov 2017a, b, c, Tilbrook *et al.* 2005, Upadhyay and Simha, 2007, Zhang *et al.* 2013).

Cracked functionally graded beams have been analyzed by Brajesh Panigrahi and Goutam Pohit (2016). The material has been functionally graded along the beam height. Clamped-clamped and clamped-free beam configurations have been considered. Dynamic analysis has been performed by modeling of cracked beams as two sub-beams connected by a mass-less rotational spring. Continuity has been assumed in longitudinal and transverse displacements at the cracked section of the beam. The effects of crack depth and crack location have been evaluated.

The post-buckling response of functionally graded beams containing an open edge crack has been investigated by Lia-Liang *et al.* (2009). It has been assumed that the material is functionally graded in the thickness direction. A detailed parametric study of the influence of the crack depth, crack location and material properties on the post-buckling behavior of the cracked beam has been carried-out.

Delamination fracture in multilayered functionally graded beams which exhibit non-linear behavior of the material has been studied by Rizov (2017a). The strain energy release rate has been analyzed assuming that the material is functionally graded in the thickness direction of each layer. The solution derived is valid for beams made of an arbitrary number of adhesively bonded layers. The delamination crack is located arbitrary between layers. Besides, the layers may have different thicknesses and material properties.

Fracture in functionally graded beams has been analyzed with taking into account the non-linear behavior of the material by Rizov (2017c). A solution to the strain energy has been derived for beams which are functionally graded in the thickness direction. Results of parametric investigations of non-linear fracture behavior have been presented.

Although many researchers have investigated fracture in functionally graded materials, there are still issues that have not been studied sufficiently. Such an issue is longitudinal fracture in beams made of non-linear elastic materials which is functionally graded along the width as well as along the length of the beam. Thus, the main purpose of the present paper was to perform a theoretical study of longitudinal fracture in such a functionally graded beam configuration.

It should be specified that the present fracture analysis is based on the small strains assumption (this assumption is frequently used in fracture analyses of functionally graded materials (Carpinteri and Pugno 2006, Upadhyay and Simha 2007)). Besides, the fracture analysis developed in the present study is valid for non-linear elastic behavior of the material. However, the analysis holds also for elastic-plastic behavior, if the external load increases only, i.e. if the beam considered undergoes active deformation (Chakrabarty 2006, Lubliner 2006).

2. Non-linear analysis of longitudinal fracture behavior

The functionally graded beam configuration shown schematically in Fig. 1 is under consideration in the present paper. The beam is clamped in section *B*. It was assumed that two

delamination cracks of length, a , are located symmetrically with respect to the centroid (it should be noted that the present study was motivated also by the fact that functionally graded materials can be built up layer by layer (Bohidar *et al.* 2014) which is a premise for appearance of longitudinal cracks between layers). The cross-section of the internal crack arm is a rectangle of width, b_1 , and height, h . The two external crack arms have rectangular cross-sections of width, b_2 and height, h . The loading consists of one bending moment, M_y , applied at the free end of the internal crack arm. Thus, the two external crack arms are free of stresses. The beam has a rectangular cross-section of width, b , and height, h . The beam length is denoted by l .

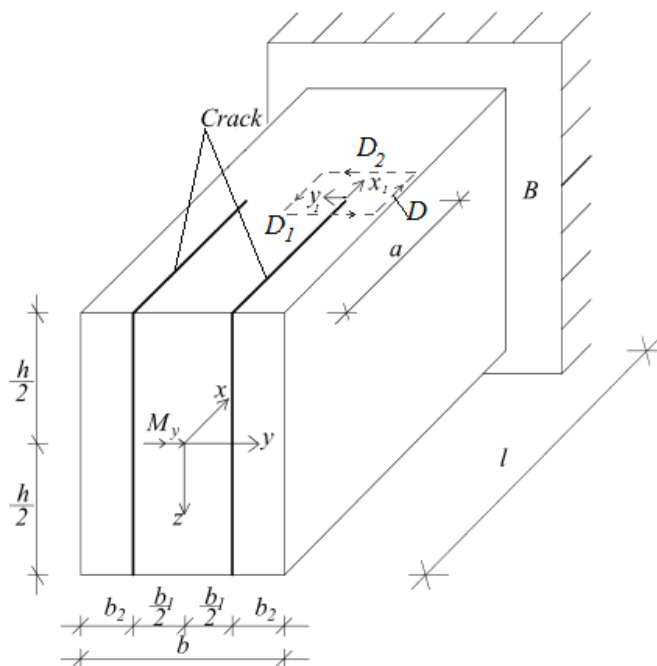


Fig. 1 Geometry and loading of a functionally graded cantilever beam configuration with two symmetric longitudinal cracks

The beam mechanical behaviour was described by the following power-law stress-strain relation (Petrov 2014)

$$\sigma = L_1 \varepsilon^{n_1} \tag{1}$$

where σ is the stress, ε is the strain, L_1 and n_1 are material properties (the non-linear stress-strain curve is shown schematically in Fig. 2).

It was assumed that the material is functionally graded along the beam width as well as along the beam length (i.e., the material is two-dimensional functionally graded). Along the beam width, the material is functionally graded symmetrically with respect to the xOz -plane. Therefore, only half of the beam, $y > 0$, was considered in the analysis (xOz is plane of symmetry). The material property, L_1 , varies continuously along the beam width from L_{1C} at the xOz -plane to pL_{1C} at the beam lateral surface according to the following bi-quadratic law

$$L_1(y) = L_{1C} \left(1 + 16 \frac{p-1}{b^4} y^4 \right), \quad p > 0 \text{ at } 0 \leq y \leq \frac{b}{2} \quad (2)$$

where the non-dimensional parameter p governs the material gradient along the beam width. Besides, L_{1C} varies linearly along the beam length from L_{1CF} in the beam free end to L_{1CB} in cross-section B (Fig. 1)

$$L_{1C} = L_{1CF} + \frac{L_{1CB} - L_{1CF}}{l} x, \quad 0 \leq x \leq l. \quad (3)$$

In other words, the material is functionally graded along x and y axes (Fig. 1).

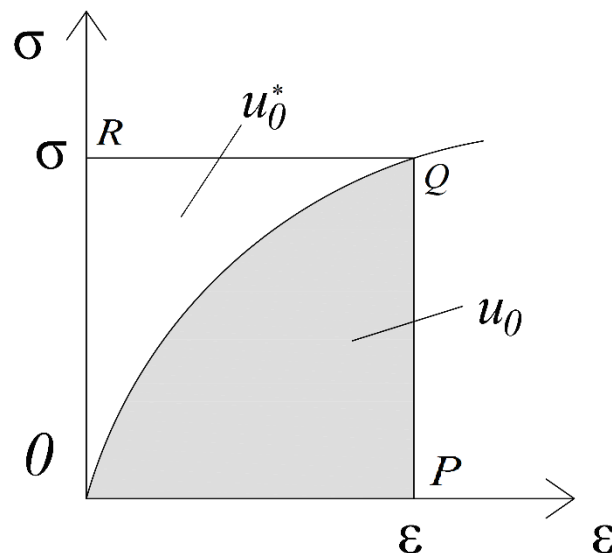


Fig. 2 Non-linear stress-strain curve (the strain energy density and the complementary strain energy density are denoted by u_0 and u_0^* , respectively)

The non-linear fracture behaviour was studied analytically in terms of the strain energy release rate, G . The following formula for G was used (Rizov 2017a)

$$G = \frac{dU^*}{hda}, \quad (4)$$

where dU^* is the increase of the complementary strain energy of the beam, da is an elementary increase of the crack length.

The complementary strain energy is zero in the two external crack arms, since they are free of stresses. Therefore, the beam complementary strain energy, U^* , was found by integration of the complementary strain energy density in the internal crack arm and in the un-cracked beam portion, $a \leq x \leq l$ (Fig. 1)

$$U^* = \int_{-\frac{h}{2}}^{\frac{h}{2}} \left[\int_0^{\frac{b_1}{2}} \left(\int_0^a u_{0i}^* dx \right) dy \right] dz + \int_{-\frac{h}{2}}^{\frac{h}{2}} \left[\int_0^{\frac{b}{2}} \left(\int_a^l u_{0u}^* dx \right) dy \right] dz \tag{5}$$

It should be specified that in (5) the integration along the y -axis was carried-out for $y>0$, because only the right-hand half of the beam cross-section was considered in the analysis due to the fact that xOz is plane of symmetry (Fig. 1). In (5), u_{0i}^* and u_{0u}^* are the complementary strain energy densities in the internal crack arm and in the un-cracked beam portion, respectively.

The complementary strain energy density is equal to the area OQR that supplements the area OPQ enclosed by the stress-strain curve to a rectangle (Fig. 2). The complementary strain energy density for the power-law stress-strain relation (1) was calculated as (Rizov 2017c)

$$u_0^* = L_1 \frac{n_1 \varepsilon^{n_1+1}}{n_1 + 1} \tag{6}$$

The strain energy density, u_0 , is equal to the area OPQ (Fig. 2). For the power-law stress-strain relation (1), the strain energy density was written as (Rizov 2017c)

$$u_0 = L_1 \frac{\varepsilon^{n_1+1}}{n_1 + 1} \tag{7}$$

The strain, ε , was analyzed by using the Bernoulli’s hypothesis for plane sections (it was assumed that this hypothesis is applicable, since the span to height ratio of the beam considered is large). Therefore, the distribution of the strains in the cross-section of the internal crack arm were written as

$$\varepsilon = \kappa_1 z, \tag{8}$$

where κ_1 is the curvature of internal crack arm (the z -axis is shown in Fig. 1). It should be noted that the Bernoulli’s hypothesis for plane sections has been widely used when analyzing fracture in functionally graded beams (Carpinteri and Pugno 2006, Upadhyay and Simha 2007). Concerning the application of Bernoulli’s hypothesis in the present analysis, it should also be mentioned that due to the fact that the beam under consideration is loaded in pure bending in vertical plane (Fig. 1), the only non-zero strain is the longitudinal strain, ε . Therefore, it follows from the small strain compatibility equations that ε is distributed linearly along the beam height.

The following equilibrium equation of internal crack arm was used in order to determine κ_1

$$M = \int_{-\frac{h}{2}}^{\frac{h}{2}} \left(\int_0^{\frac{b_1}{2}} \sigma z dy \right) dz, \tag{9}$$

where

$$M = \frac{1}{2} M_y. \tag{10}$$

It should be specified that the factor of $\frac{1}{2}$ in formula (14) accounts for the fact that only half of the beam was analyzed due to the symmetry (Fig. 1). The following equation with unknown κ_1 was obtained after substitution of (1), (2) and (8) in (9)

$$M = L_{1C} \kappa_1^{n_1} \frac{b_1}{2(n_1 + 2)} \left[\left(\frac{h}{2} \right)^{n_1+2} - \left(-\frac{h}{2} \right)^{n_1+2} \right] \left(1 + b_1^4 \frac{p-1}{5b^4} \right). \quad (11)$$

Eq. (11) was solved with respect to κ_1 . It was obtained

$$\kappa_1 = \left\{ \frac{2(n_1 + 2)M}{L_{1C} b_1 \left[\left(\frac{h}{2} \right)^{n_1+2} - \left(-\frac{h}{2} \right)^{n_1+2} \right] \left(1 + b_1^4 \frac{p-1}{5b^4} \right)} \right\}^{\frac{1}{n_1}}, \quad (12)$$

where L_{1C} and M are determined by (3) and (10), respectively.

Clearly, at $n_1=1$ the non-linear stress-strain relation (1) transforms into the Hooke's law. This means that at $n_1=1$ Eq. (12) should transform in the formula for curvature of linear-elastic beam. Indeed, by substitution of $n_1=1$, $p=1$ and $L_{1C}=E$ (here E is the modulus of elasticity) in (12), we derived

$$\kappa_1 = \frac{24M}{Eb_1 h^3}, \quad (13)$$

which coincides with the formula for curvature of linear-elastic homogeneous beam of width, $b_1/2$, and height, h .

Eq. (12) was used also to calculate the curvature, κ , of the un-cracked beam portion. For this purpose, b_1 was replaced with b .

Formulae (1), (2), (8) and (12) were substituted in (6) to calculate the complementary strain energy density in the internal crack arm. It was obtained

$$u_0^* = L_{1C} \left(1 + 16 \frac{p-1}{b^4} y^4 \right) \frac{n_1 z^{n_1+1}}{n_1 + 1} \left\{ \frac{2(n_1 + 2)M}{L_{1C} b_1 \left[\left(\frac{h}{2} \right)^{n_1+2} - \left(-\frac{h}{2} \right)^{n_1+2} \right] \left(1 + b_1^4 \frac{p-1}{5b^4} \right)} \right\}^{\frac{n_1+1}{n_1}}. \quad (14)$$

Likewise, the complementary strain energy density in the un-cracked beam portion, u_{0u}^* , was found by substitution of (1), (2) and in (6).

$$\mathcal{E} = \kappa z, \quad (15)$$

In this way, the following formula was obtained

$$u_{0u}^* = L_{1C} \left(1 + 16 \frac{p-1}{b^4} y^4 \right) \frac{n_1 z^{n_1+1}}{n_1 + 1} \left\{ \frac{2(n_1 + 2)M}{L_{1C} b \left[\left(\frac{h}{2} \right)^{n_1+2} - \left(-\frac{h}{2} \right)^{n_1+2} \right] \left(1 + \frac{p-1}{5} \right)} \right\}^{\frac{n_1+1}{n_1}} \quad (16)$$

The expression derived by substituting of (5), (14) and (16) in (4) was doubled, because there are two symmetric longitudinal cracks in the beam under consideration (Fig. 1). In this way, we obtained the following formula for the strain energy release rate

$$G = \frac{n_1(n_1 + 2)^{\frac{1}{n_1}} M_y^{\frac{n_1+1}{n_1}}}{h(n_1 + 1) \left[\left(\frac{h}{2} \right)^{n_1+2} - \left(-\frac{h}{2} \right)^{n_1+2} \right]^{\frac{1}{n_1}} \left(L_{1CF} + \frac{L_{1CB} - L_{1CF}}{l} a \right)^{\frac{1}{n_1}}} \left\{ \frac{1}{b_1^{\frac{1}{n_1}} \left[1 + \frac{b_1^4(p-1)}{5b^4} \right]^{\frac{1}{n_1}}} - \frac{1}{b^{\frac{1}{n_1}} \left(1 + \frac{p-1}{5} \right)^{\frac{1}{n_1}}} \right\} \quad (17)$$

In order to verify (17), an additional fracture analysis was developed by applying the *J*-integral approach (Broek 1986). The *J*-integral was solved by using an integration contour, *D*, shown by dashed line in Fig. 1. The *J*-integral in the external crack arms is zero. Thus, the *J*-integral solution was expressed as

$$J = J_{D_1} + J_{D_2} \quad (18)$$

where *J*_{*D*₁} and *J*_{*D*₂} are the *J*-integral values in segments *D*₁ and *D*₂, respectively (*D*₁ and *D*₂ coincide with the right-hand half of the cross-section of the internal crack arm and the right-hand half of the cross-section of the un-cracked beam portion, respectively).

The *J*-integral in segments *D*₁ was written as

$$J_{D_1} = \int_{D_1} \left[u_0 \cos \alpha - \left(p_{x_1} \frac{\partial u}{\partial x_1} + p_{y_1} \frac{\partial v}{\partial x_1} \right) \right] ds \quad (19)$$

where α is the angle between the outwards normal vector to the contour of integration and the crack direction, p_{x_1} and p_{y_1} are the components of stress vector, u and v are the components of displacement vector with respect to the crack tip coordinate system x_1y_1 (x_1 is directed along the crack), ds is a differential element along the contour.

In segment, *D*₁, of the integration contour, the components of the *J*-integral were found as

$$p_{x_1} = -\sigma = -L_1 \varepsilon^{n_1}, \quad p_{y_1} = 0 \quad (20)$$

$$ds = dy, \cos \alpha = -1, \tag{21}$$

where y varies in the interval $[0, b_1/2]$.

The partial derivative, $\partial u/\partial x_1$, in (19) is expressed as

$$\frac{\partial u}{\partial x_1} = \varepsilon = z\kappa_1. \tag{22}$$

By substituting of (1), (2), (7), (8), (20), (21) and (22) in (19), we derived

$$J_{D_1} = L_{1C} \left(\frac{b_1}{2} + \frac{p-1}{b^4} \frac{b_1^5}{10} \right) \frac{n_1 z^{n_1+1}}{n_1+1} \left\{ \frac{2(n_1+2)M}{L_{1C} b_1 \left[\left(\frac{h}{2} \right)^{n_1+2} - \left(-\frac{h}{2} \right)^{n_1+2} \right] \left(1 + b_1^4 \frac{p-1}{5b^4} \right)} \right\}^{\frac{n_1+1}{n_1}}, \tag{23}$$

where z varies in the interval $[-h/2, h/2]$. In (23), L_{1C} is obtained by (3) at $x=a$.

The solution of the J -integral in segment, D_2 , of the integration contour was found by (23). For this purpose, b_1 was replaced with b . Besides, the sign of (23) was set to “minus” because the integration contour is directed upwards in segment, D_2 .

The expression obtained by substituting of J_{D_1} and J_{D_2} in (18) was doubled in view of the symmetry (Fig. 1). In this way, we derived

$$J = L_{1C} \left(b_1 + \frac{p-1}{b^4} \frac{b_1^5}{5} \right) \frac{n_1 z^{n_1+1}}{n_1+1} \left\{ \frac{2(n_1+2)M}{L_{1C} b_1 \left[\left(\frac{h}{2} \right)^{n_1+2} - \left(-\frac{h}{2} \right)^{n_1+2} \right] \left(1 + b_1^4 \frac{p-1}{5b^4} \right)} \right\}^{\frac{n_1+1}{n_1}} -$$

$$- L_{1C} \left(b + b \frac{p-1}{5} \right) \frac{n_1 z^{n_1+1}}{n_1+1} \left\{ \frac{2(n_1+2)M}{L_{1C} b \left[\left(\frac{h}{2} \right)^{n_1+2} - \left(-\frac{h}{2} \right)^{n_1+2} \right] \left(1 + \frac{p-1}{5} \right)} \right\}^{\frac{n_1+1}{n_1}}, \tag{24}$$

where L_{1C} is obtained by (3) at $x=a$.

Formula (24) expresses the distribution of the J -integral value along the crack front. The average value of the J -integral along the crack front was written as

$$J_{AV} = \frac{1}{h} \int_{-\frac{h}{2}}^{\frac{h}{2}} J dz. \tag{25}$$

The fact that the solution of the J -integral obtained by substituting of (24) in (25) matches exactly the strain energy release rate (17) is a verification of the non-linear fracture analysis developed in the present paper.

3. Numerical results

The influence of material gradient, crack location along the beam width, crack length and non-linear material behavior on the fracture was analyzed. For this purpose, the strain energy release rate was calculated by using formula (17). It was assumed that $b=0.008$ m, $h=0.009$ m and $M_y=10$ Nm. The strain energy release rate was presented in non-dimensional form by using the formula $G_N=G/(L_{1CF}h)$. In the calculations, the material property L_{1CF} was kept constant. Thus, the parameter p was varied in order to obtain various material gradients along the beam width (refer to formula (2)). The crack length and the crack location along the beam width were characterized by a/l and b_1/b ratios, respectively. The strain energy release rate was plotted in non-dimensional form against the parameter p for $b_1/b=0.3, 0.5$ and 0.7 at $L_{1CB}/L_{1CF}=1$ and $a/l=0.3$ in Fig. 3.

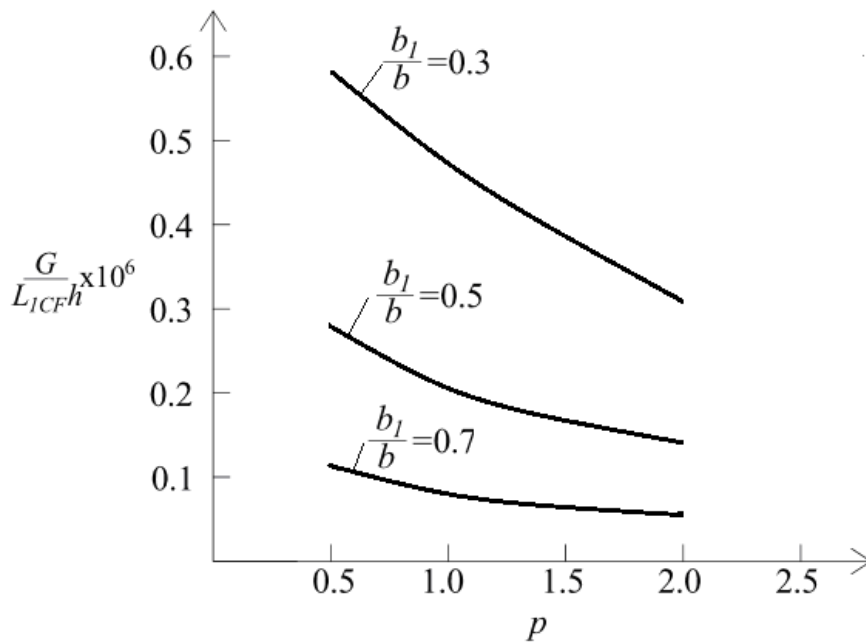


Fig. 3 The strain energy release rate in non-dimensional form plotted against the parameter p for $b_1/b=0.3, 0.5$ and 0.7

The diagrams in Fig. 3 indicate that the strain energy release rate decreases with increasing the parameter p . This finding was explained with the increase of the beam stiffness. It can also be observed in Fig. 3 that the strain energy release rate decreases with increasing b_1/b ratio. This finding was attributed to the increase of the stiffness of the internal crack arm (the two external crack arms are free of stresses).

The effects of crack length and non-linear material behavior on the fracture were also evaluated. For this purpose, calculations of G were performed at various a/l ratios. The strain energy release rate obtained from these calculations is shown in non-dimensional form in Fig. 4 as a function of a/l ratio for $L_{1CB}/L_{1CF}=2$, $p=0.5$ and $b_1/b=0.5$. One can observe in Fig. 4 that the strain energy release rate decreases with increasing the crack length (this finding was attributed to the fact that at $L_{1CB}/L_{1CF}=2$ the material property, L_{1C} , in the beam cross-section in which the crack front is located increases with increasing the crack length).

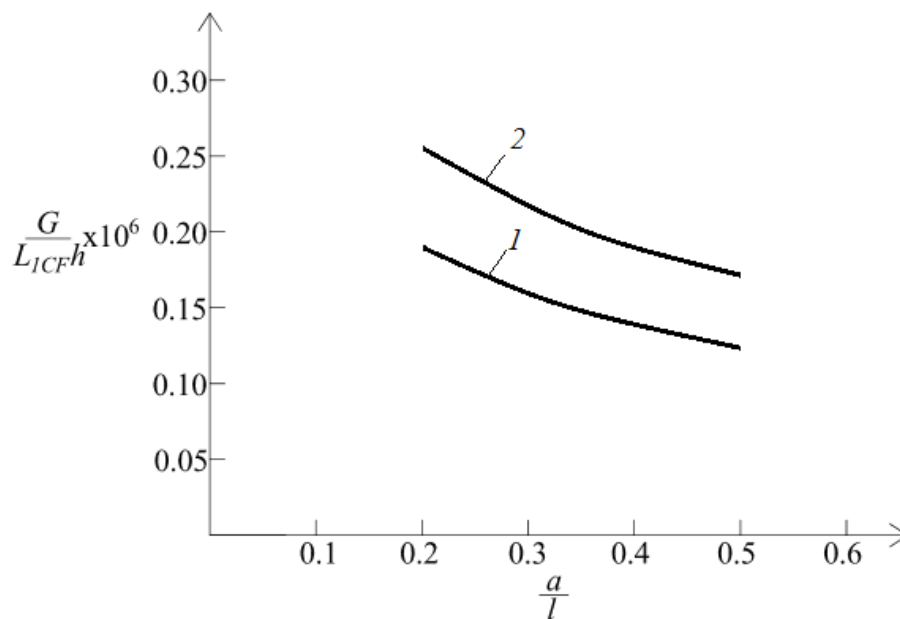


Fig. 4 The strain energy release rate in non-dimensional form plotted against a/l ratio (curve 1-at linear-elastic behavior of the material, curve 2-at non-linear behavior of the material)

In order to evaluate the effect of material non-linearity on the fracture, the strain energy release rate calculated assuming linear-elastic behavior of the functionally graded material was plotted also as a function of a/l ratio in Fig. 4 for comparison with the non-linear solution (the linear-elastic solution was derived by substituting of $n_1=1$ in (17)). It can be observed in Fig. 4 that the strain energy release rate increases when the non-linear behavior of the material is taken into account. This finding indicates that the material non-linearity has to be considered in fracture mechanics based safety design of functionally graded structural members.

4. Conclusions

An analytical investigation of fracture in a functionally graded cantilever beam with two longitudinal cracks located symmetrically with respect to the centroid was performed with taking into account the non-linear behavior of the material. It was assumed that the material is functionally graded along the beam width as well as along the beam length. The beam mechanical

behavior was described by a power-law stress-strain relation. A non-linear analytical solution was derived for the strain energy release rate. In order to verify the solution, an additional fracture analysis was developed by applying the J -integral approach. The influence of the material gradient, crack location along the beam width, crack length and material non-linearity on the longitudinal fracture behavior was analyzed. It was found that the material non-linearity leads to increase of the strain energy release rate. Therefore, the non-linear behavior of material has to be taken into account in fracture mechanics based safety design of functionally graded structural members. The solution derived is very useful for parametric studies of longitudinal fracture with considering the material non-linearity. The results obtained can be applied for optimization of the beam structure with respect to its fracture performance. For instance, the analysis performed indicates that the strain energy release rate can be significantly reduced by choosing suitable material gradients in both width and length directions of the functionally graded beam.

References

- Ait Amar Meziane, M., Abdelaziz, H.H. and Tounsi, A. (2014), "An efficient and simple refined theory for buckling and free vibration of exponentially graded sandwich plates under various boundary conditions", *J. Sandw. Struct. Mater.*, **16**(3), 293-318.
- Ait Atmane, H., Tounsi, A. and Bernard, F. (2015), "Effect of thickness stretching and porosity on mechanical response of a functionally graded beams resting on elastic foundations", *Int. J. Mech. Mater. Des.*, **13**(1), 71-84.
- Bellifa, H., Benrahou, K.H., Hadji, L., Houari, M.S.A. and Tounsi, A. (2016), "Bending and free vibration analysis of functionally graded plates using a simple shear deformation theory and the concept the neutral surface position", *J. Braz. Soc. Mech. Sci. Eng.*, **38**(1), 265-275.
- Bohidar, S.K., Sharma, R. and Mishra, P.R. (2014), "Functionally graded materials: A critical review", *Int. J. Res.*, **1**(7), 289-301.
- Bourada, M., Kaci, A., Houari, M.S.A. and Tounsi, A. (2015), "A new simple shear and normal deformations theory for functionally graded beams", *Steel Compos. Struct.*, **18**(2), 409-423.
- Brajesh, P. and Goutam, P. (2016), "Nonlinear modelling and dynamic analysis of cracked Timoshenko functionally graded beams based on neutral surface approach", *J. Mech. Eng. Sci.*, **230**(9), 1468-1497.
- Broek, D. (1986), *Elementary Engineering Fracture Mechanics*, Springer.
- Carpinteri, A. and Pugno, N. (2006), "Cracks in re-entrant corners in functionally graded materials", *Eng. Fract. Mech.*, **73**(6), 1279-1291.
- Chakrabarty, J. (2006), *Theory of Plasticity*, Elsevier Butterworth-Heinemann, Oxford.
- Ebrahimi, F. and Barati, M.R. (2016a), "Dynamic modeling of a thermo-piezo-electrically actuated nanosize beam subjected to a magnetic field", *Appl. Phys. A*, **122**(4), 1-18.
- Ebrahimi, F. and Barati, M.R. (2016c), "Magnetic field effects on buckling behavior of smart size-dependent graded nanoscale beams", *Eur. Phys. J. Plus*, **131**(7), 1-14.
- Ebrahimi, F. and Barati, M.R. (2016e), "Buckling analysis of smart size-dependent higher order magneto-electro-thermo-elastic functionally graded nanosize beams", *J. Mech.*, **33**(1), 23-33.
- Ebrahimi, F. and Barati, M.R. (2016f), "A nonlocal higher-order shear deformation beam theory for vibration analysis of size-dependent functionally graded nanobeams", *Arab. J. Sci. Eng.*, **41**(5), 1679-1690.
- Ebrahimi, F. and Barati, M.R. (2016d), "Electromechanical buckling behavior of smart piezoelectrically actuated higher-order size-dependent graded nanoscale beams in thermal environment", *Int. J. Smart Nano Mater.*, **7**(2), 69-90.
- Ebrahimi, F. and Barati, M.R. (2016g), "Buckling analysis of nonlocal third-order shear deformable functionally graded piezoelectric nanobeams embedded in elastic medium", *J. Braz. Soc. Mech. Sci. Eng.*,

- 39**(3), 937-952.
- Ebrahimi, F. and Farzamandnia, N. (2016), "Thermo-mechanical vibration analysis of sandwich beams with functionally graded carbon nanotube-reinforced composite face sheets based on a higher-order shear deformation beam theory", *Mech. Adv. Mater. Struct.*, **24**(10), 820-829.
- Ebrahimi, F. and Jafari, A. (2016), "A higher-order thermomechanical vibration analysis of temperature-dependent FGM beams with porosities", *J. Eng.*
- Ebrahimi, F. and Salari, E. (2015), "A semi-analytical method for vibrational and buckling analysis of functionally graded nanobeams considering the physical neutral axis position", *CMES Comput. Model. Eng. Sci.*, **105**(2), 151-181.
- Ebrahimi, F. and Shafiei, N. (2016), "Influence of initial shear stress on the vibration behavior of single-layered graphene sheets embedded in an elastic medium based on Reddy's higher-order shear deformation plate theory", *Mech. Adv. Mater. Struct.*, **24**(9), 761-772.
- Ebrahimi, F. and Barati, M.R. (2016b), "Vibration analysis of smart piezoelectrically actuated nanobeams subjected to magneto-electrical field in thermal environment", *J. Vibr. Contr.*, **24**(3), 549-564.
- Ebrahimi, F., Javad, E. and Ramin, B. (2016), "Thermal buckling of FGM nanoplates subjected to linear and nonlinear varying loads on Pasternak foundation", *Adv. Mater. Res.*, **5**(4), 245-261.
- Erdogan, F. (1995), "Fracture mechanics of functionally graded materials", *Comp. Eng.*, **5**(7), 753-770.
- Gasik, M.M. (2010), "Functionally graded materials: Bulk processing techniques", *Int. J. Mater. Prod. Technol.*, **39**(1-2), 20-29.
- Hadji, L. (2017), "Analysis of functionally graded plates using a sinusoidal shear deformation theory", *Smart Struct. Syst.*, **19**(4), 441-448.
- Hadji, L., Khelifa, Z., Daouadji, T.H. and Bedia, E.A. (2015), "Static bending and free vibration of FGM beam using an exponential shear deformation theory", *Coupled Syst. Mech.*, **4**(1), 99-114.
- Hadji, L., Zouatnia, N. and Kassoul, A. (2017), "Wave propagation in functionally graded beams using various higher-order shear deformation beams theories", *Struct. Eng. Mech.*, **62**(2), 143-149.
- Hirai, T. and Chen, L. (1999), "Recent and prospective development of functionally graded materials in Japan", *Mater. Sci. Forum*, **308-311**(4), 509-514.
- Koizumi, M. (1993), "The concept of FGM ceramic trans", *Function. Grad. Mater.*, **34**(1), 3-10.
- Ke, L.L., Yang, J. and Kitiporncha, S. (2009), "Postbuckling analysis of edge cracked functionally graded Timoshenko beams under end shortening", *Compos. Struct.*, **90**, 152-160.
- Lu, C.F., Lim, C.W. and Chen, W.Q. (2009), "Semi-analytical analysis for multi-dimensional functionally graded plates: 3-D elasticity solutions", *Int. J. Numer. Meth. Eng.*, **79**(3), 25-44.
- Lubliner, J. (2006), *Plasticity Theory*, Revised Edition, University of California, Berkeley, California, U.S.A.
- Markworth, A.J., Ramesh, K.S. and Parks, J.W.P. (1995), "Review: Modeling studies applied to functionally graded materials", *J. Mater. Sci.*, **30**(3), 2183-2193.
- Mortensen, A. and Suresh, S. (1995), "Functionally graded metals and metal-ceramic composites: Part 1 processing", *Int. Mater. Rev.*, **40**(6), 239-265.
- Naser, S.A.H. and Sami, T.A. (2017), "Transient thermo-mechanical response of a functionally graded beam under the effect of a moving heat source", *Adv. Mater. Res.*, **6**(1), 27-43.
- Nemat-Allal, M.M., Ata, M.H., Bayoumi, M.R. and Khair-Eldeen, W. (2011), "Powder metallurgical fabrication and microstructural investigations of aluminum/steel functionally graded material", *Mater. Sci. Appl.*, **2**(5), 1708-1718.
- Neubrand, A. and Rödel, J. (1997), "Gradient materials: An overview of a novel concept", *Zeit. f. Met.*, **88**(4), 358-371.
- Paulino, G.C. (2002), "Fracture in functionally graded materials", *Eng. Fract. Mech.*, **69**(5), 1519-1530.
- Petrov, V.V. (2014), *Non-Linear Incremental Structural Mechanics*, M.: Infra-Injeneria.
- Rizov, V.I. (2017b), "Non-linear analysis of delamination fracture in functionally graded beams", *Coupled Syst. Mech.*, **6**(1), 97-111.
- Rizov, V.I. (2017a), "Delamination fracture in a functionally graded multilayered beam with material nonlinearity", *Arch. Appl. Mech.*, **87**(6), 1037-1048.

- Rizov, V.I. (2017c), “An analytical solution to the strain energy release rate of a crack in functionally graded nonlinear elastic beams”, *Eur. J. Mech. A/Sol.*, **65**, 301-312.
- Tilbrook, M.T., Moon, R.J. and Hoffman, M. (2005), “Crack propagation in graded composites”, *Compos. Sci. Technol.*, **65**(2), 201-220.
- Upadhyay, A.K. and Simha, K.R.Y. (2007), “Equivalent homogeneous variable depth beams for cracked FGM beams; compliance approach”, *Int. J. Fract.*, **144**(2), 209-213.
- Zhang, H., Li, X.F., Tang, G.J. and Shen, Z.B. (2013), “Stress intensity factors of double cantilever nanobeams via gradient elasticity theory”, *Eng. Fract. Mech.*, **105**(1), 58-64.

CC